Distributed Jamming Method for STAP Radar Based on Algorithm of Improved MOEA/D-PBI

Wenbo Yang, Gaogao Liu(✉), Dongjie Huang, and Minhua Zheng

Xidian University, Xi'an, China
hywbwyang@163.com, ggliu@xidian.edu.cn, 546669844@qq.com, 906383787@qq.com

Abstract. In modern warfare, the role of airborne early warning aircraft is becoming more and more significant. The airborne early warning radar can accurately detect moving targets in a chaotic environment. Its suppression of strong clutter and jamming by radar is mainly through space-time adaptive processing (STAP) technology to achieve. The STAP algorithm uses the two domains of time and space to perform two-dimensional joint processing on the echo data, adaptively forming a notch that matches the clutter and jamming, and its excellent jamming suppression capability increases the difficulty of radar countermeasures. In this case, it is very necessary to conduct a comprehensive jamming study about the technology. At present, relevant jamming methods at home and abroad are still in the preliminary research stage. In this paper, we take genetic algorithm as an example, and a new distributed jamming method for STAP radar based on improved penalty-based boundary intersection decomposition multiobjective evolutionary algorithm (MOEA/D-PBI) is introduced in the many-to-many confrontation. Through simulation experiments, the optimized distributed jamming scheme is compared with the distributed jamming scheme before optimization, verifying the feasibility of the method proposed in this paper, which simplifies the problem of jamming resource allocation and realizes a fast search for the optimal allocation strategy, and complete real-time jamming decision-making on the battlefield.

Keywords: Improved penalty-based boundary intersection · Distributed jamming · Genetic algorithm

1 Introduction

Compared with the simpler clutter suppression process of ground-based radars, the signal detection environment faced by airborne radars is more complicated. The radar's suppression of strong clutter and jamming is mainly achieved through space-time adaptive processing (STAP) technology [1]. STAP radar has strong adaptability and can deal with strong clutter and conventional jamming effectively. It can be seen that the STAP radar with superior clutter suppression performance makes it difficult for the interfering side to implement countermeasures [2]. At present, the field of STAP radar jamming is in its infancy. Current jamming research on the STAP algorithm only focuses on designing

X. Wang et al. (Eds.): AICON 2021, LNICST 396, pp. 402–414, 2021.
https://doi.org/10.1007/978-3-030-90196-7_34

effective jamming patterns, thereby destroying the independent and identical distribution conditions of the training samples in the STAP algorithm [1]. Therefore, the jamming research on the signal of STAP radar is an effective means to suppress the performance of STAP radar, and it is of great significance to cover the jammer's target.

The traditional jamming method against STAP radar is single-point source main lobe jamming [3]. In the long-distance support sidelobe jamming, because the number of jammers is small and the target is far away, it will be suppressed by the space-time two-dimensional processing, and will not bring a certain threat to the target detection [2]. At the same time, radar jamming resource allocation scenarios are often for jammers against a single radar. When the number of radars increases, considering that a single jammer will be affected by various factors such as jamming pattern, jamming power and frequency band, the effectiveness of jamming is difficult to guarantee [4].

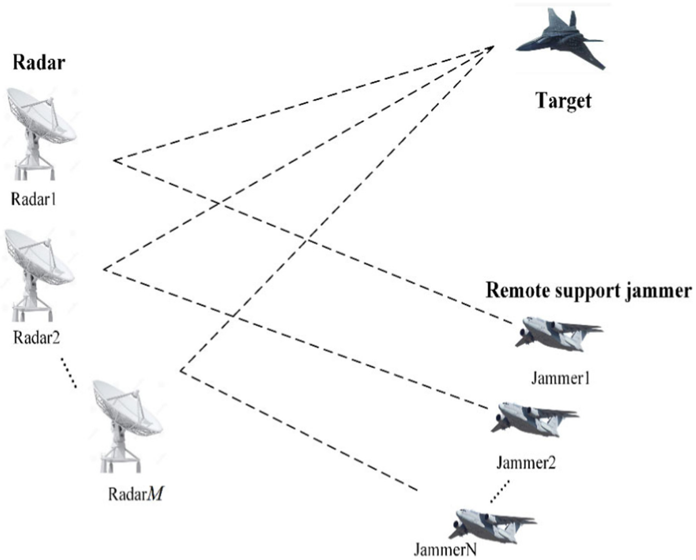

Fig. 1. Many-to-many jamming situation.

In addition, due to the many-to-many jamming situation (Fig. 1), the research on the countermeasures between the radar network platform and the cooperative jamming system becomes more and more important. How to reasonably allocate the jamming resources under the existing multiple jammers to obtain a more accurate jamming decision, which has a strong guide for the action direction of the interferer [4]. Since the radar countermeasures process is affected by many factors such as environment and man-made factors, different strategies will have different jamming effects. If rely on traditional experience to make decisions, it will be biased.

To overcome above drawbacks, a distributed jamming method for STAP radar based on improved penalty-based boundary intersection decomposition multiobjective evolutionary algorithm (MOEA/D-PBI) is proposed in this paper to effectively allocate jamming resources, thereby realizing effective jamming to STAP radars. This method takes into consideration the landscape of each subproblem and adaptively adjust each subproblem's penalty value during the search. Our experimental study validate the effectiveness of the proposed method. The rest of this paper is organized as follows. Section 2 presents traditional work and illustrates the improved PBI approach. The proposed distributed jamming method is described in Sect. 3. Experimental studies are presented in Sect. 4. Finally, Sect. 5 concludes this paper.

2 MOEA/D-PBI Algorithm

2.1 MOEA/D Algorithm

Multiobjective evolutionary algorithm based on decomposition (MOEA/D) used in this paper needs to decompose the MOP under consideration [5, 6]. MOEA/D employs a set of predefined weight vectors that uniformly partition the entire objective space to specify a number of search directions, and defines a single-objective problem or a multiobjective subproblem by decomposition approaches for each search direction. For each search direction, MOEA/D also specifies$T$ closest neighbours before-hand, which helps to efficiently solve the associated single-objective problem in a collaborative manner [7]. During the course of search, mating selection and replacement are considered among solutions associated with the T neighbouring search directions. MOEA/D is a steady-state algorithm and up-dates solutions one by one, so it approximates the true Pareto-optimal front (POF) quickly [8].

The algorithm framework of distributed jamming method based on improved MOEA/D-PBI is proposed in Sect. 2.3. Any decomposition approaches can serve this purpose. In this paper, we only study the following decomposition approach in our experimental studies.

2.2 Traditional PBI Review

Decomposition approaches play a key role in converting a multiobjective optimization problem (MOP) into a number of scalar optimizations subproblems in decomposition-based multiobjective evolutionary algorithms (MOEAs). Several recent MOP decomposition methods such as Normal-Boundary Intersection Method [9] and Normalized Normal Constraint Method [10] can be classified as the boundary intersection (BI) approaches. They were designed for a continuous MOP. Under some regularity conditions, the Pareto front (PF) of a continuous MOP is part of the most top right boundary of its attainable objective set. Geometrically, these BI approaches aim to find intersection points of the most top boundary and a set of lines. If these lines are evenly distributed in a sense, one can expect that the resultant intersection points provide a good approximation to the whole PF. These approaches are able to deal with nonconcave PFs.

The traditional PBI approach has its advantages in obtaining a good distribution of solutions in the objective space [7] and handling many objective problems, but its performance is very sensitive to the setting of the penalty factor [8]. The specific decomposition method based on traditional PBI is as follows.

$$\text{minimize}\left\{g^{pbi}\left(x\middle|\lambda, z^*\right) = d_1 + \theta d_2\right\}, x \in \Theta \tag{1}$$

Where, minimize{·} is minimum operation and x is variable to be optimized. As shown in Fig. 2, d_1 is the distance between z^* and y, d_2 is the distance between $F(x)$ and L. $z^* = \left(z_1^*, z_2^*, \cdots, z_i^* \cdots, z_N^*\right)^T$ is the reference point. λ is a weight vector. Θ is decision space. $\theta > 0$ is preset penalty parameter.

According to the following formula (2), calculate d_1

$$d_1 = \frac{\|(F(x) - z^*)^T \lambda\|}{\|\lambda\|} \tag{2}$$

According to the following formula (3), calculate d_2

$$d_2 = \|F(x) - \left(z^* + d_1 \frac{\lambda}{\|\lambda\|}\right)\| \tag{3}$$

A brief illustration of the traditional PBI approach is shown in Fig. 2. It is easy to see that θ takes the responsibility for balancing convergence (measured by d_1) and diversity (measured by d_2). By minimizing g^{pbi}, the PBI approach drives the solution toward the obtained idea point z^* and stresses the closeness of the solution to the predefined search direction. If possible, the traditional PBI approach will try to locate a solution on the intersection of each search direction and the true POF when a set of uniformly-distributed search directions are given.

However, one has to set the value of the penalty factor. It is well-known that a too large or too small penalty factor θ will worsen the performance of a penalty method. These disadvantages limit the wide application of the algorithm.

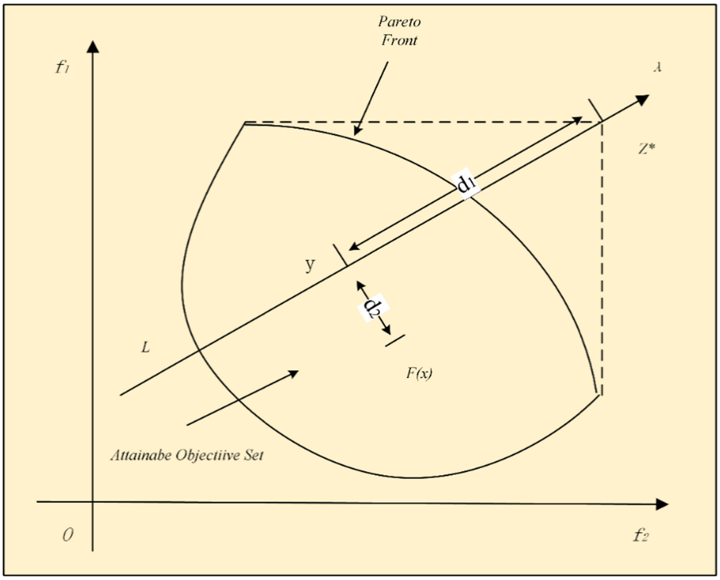

Fig. 2. Brief illustration of the traditional PBI approach.

In this paper, our main purpose is to study the efficiency and feasibility of the algorithm framework. Therefore, we only use the following improved decomposition approach in the experimental studies.

2.3 Improved PBI Introduction

According to formula (1), in order to overcome the sensitivity caused by θ. Consider adjusting the penalty value θ_i of the ith subproblem in each generation of search and optimization [11, 12].

$$\theta_i^{t+1} = \begin{cases} min_{1 \le j \le N}\left\{\theta_j^t\right\}, \ if\ similar\ environments, \\ \theta_i^t + \Delta\theta_i, \ otherwise. \end{cases} \tag{4}$$

Where θ_i^t is the θ_i at generation t, and $\Delta\theta_i$ is calculated by:

$$\Delta\theta_i = sgn(\alpha - 1) \cdot \alpha \cdot \theta_i^{min} \tag{5}$$

Where $\alpha = \frac{d_{i,2}}{\overline{d_2}}$ in which $\overline{d_2}$ is the average of all $d_{i,2}$ values. $sgn(\cdot)$ is the sign function, and θ_i^{min} is the minimum allowable value of θ_i. Correspondingly, θ_i^{max} is the maximum allowable value of θ_i.

Then, θ_i^{t+1} obtained from formula (4) should be repaired to keep its value in the range $\left[\theta_i^{min}, \theta_i^{max}\right]$, which can be achieved by:

$$\theta_i^{t+1} = \begin{cases} \theta_i^{\min}, \theta_i^{t+1} < \theta_i^{\min} \\ \theta_i^{\max}, \theta_i^{t+1} > \theta_i^{\max} \\ \theta_i^{t+1}, \ \ else \end{cases} \tag{6}$$

Where the initial penalty value is set to $\theta_i^1 = \theta_i^{min}$ for all the subproblems in our experimental studies.

Seen from formula (4), when subproblems have different environments, their penalties depend on the diversity of individuals. If the individual's $d_{i,2}$ is greater than the average $\overline{d_2}$, the subproblem can increase the penalty value to emphasize the proximity to the corresponding search direction, and vice versa. When all subproblems have very similar scenarios, they can have the same penalty value, which is actually the minimum of all θ_i^t values. But we cannot judge in advance whether all subproblems have similar scenarios. Therefore, it requires a scenario estimator to judge the similarity of the subproblems.

The definition of the environment similarity of the subproblems is given below: If the optimal solutions of the subproblems have similar $d_{i,1}$, the subproblems are said to have similar situations. In the search process, when all the $d_{i,2}$ values are very small, consider the $d_{i,1}$ values. If all the $d_{i,1}$ values are similar, then the sub-problems can be considered to be similar in landscape. A 2-objective case of the judgement condition of environment similarity is presented in Fig. 3. The similarity condition is expressed as:

$$\overline{d_2} < \delta \wedge d_{max,1} < \sqrt{M} \cdot d_{min,1} \tag{7}$$

Where δ is a very small non-negative threshold value. For simplicity, δ is set to 10^{-3}, indicating all $d_{i,2}$ values are very small and good population diversity has been achieved. $d_{min,1}$ and $d_{max,1}$ are the minimum and maximum value of $d_{i,1}$, respectively, and M is the number of objectives.

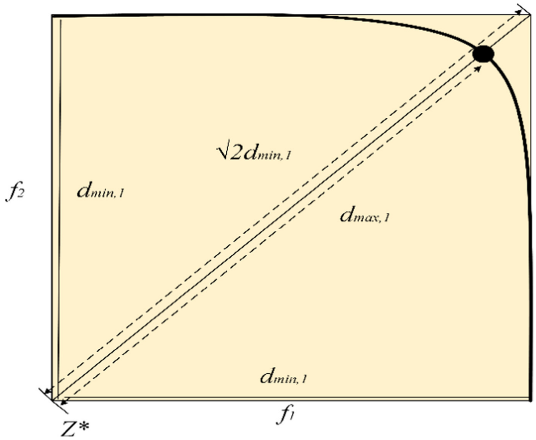

Fig. 3. An illustration of the condition of environment similarity in the 2 objectives case.

3 Distributed Jamming Method

In this paper, we propose a new distributed jamming method based on improved PBI decomposition approach.

– **Step 0: Initialization:**

- First of all, to determine the threat level $\omega_{r1}, \omega_{r2}, ..., \omega_{ri}, ..., \omega_{rN}$ of each radar, the reconnaissance equipment must master the parameter information of the N intercepted radars set $R = [R_1, R_2, ..., R_i, ..., R_N]$. Among them, the key parameters include, but are not limited to the signal bandwidth $B_1, B_2, ..., B_i, ..., B_N$ of each radar pulse signal, the carrier frequency $f_{c1}, f_{c2}, ..., f_{ci}, ..., f_{cN}$ of each radar pulse signal, the transmission power $P_{r1}, P_{r2}, ..., P_{ri}, ..., P_{rN}$ of each radar pulse signal, etc. N represents the number of radars, and the value is a positive integer; R_i represents the ith radar, i is the radar index, and it's value is a positive integer; ω_{ri} represents the threat level of the ith radar, and the value is a real number within 0–1; B_i represents the bandwidth of the ith radar, and the value is a positive integer; f_{ci} represents the carrier frequency of the ith radar, and the value is positive integer; P_{ri} represents the transmit power of the ith radar;
- Consider setting up M jammers $J = \left[J_1, J_2, ..., J_j, ..., J_M\right]$, where J_j means the j th jammer, M is the number of jammers, $M > 0$;
- A mathematical model of multiobjective jamming resource scheduling considering decision variables such as jamming pattern and jamming power. The objective function is shown in the following formula (8).

$$F(x):\begin{cases} f_1(x) = \omega_{r1}\cdot(a_{11}s_{11}p_{11} + a_{21}s_{21}p_{21} + \cdots + a_{M1}s_{M1}p_{M1}) \\ f_2(x) = \omega_{r2}\cdot(a_{12}s_{12}p_{12} + a_{22}s_{22}p_{22} + \cdots + a_{M2}s_{M2}p_{M2}) \\ \vdots \\ f_i(x) = \omega_{ri}\cdot\left(a_{1i}s_{1i}p_{1i} + a_{2i}s_{2i}p_{2i} + \cdots + a_{ji}s_{ji}p_{ji}\cdots + a_{Mi}s_{Mi}p_{Mi}\right) \\ \vdots \\ f_N(x) = \omega_{rN}\cdot(a_{1N}s_{1N}p_{1N} + a_{2N}s_{2N}p_{2N} + \cdots + a_{MN}s_{MN}p_{MN}) \end{cases} \quad (8)$$

Where $F(x)$ is the set of $f_1(x), f_2(x), \ldots, f_N(x)$, $f_i(x)$ represents the jamming target function corresponding to the ith radar. a_{ji} is the space-time jamming factor of the jth jammer to the ith radar, and its value is a real number within 0–1. p_{ji} is the normalized jamming power of the jth jammer to the ith radar, and its value is a real number within 0–1. s_{ji} is the jamming pattern used by the jth jammer to interfere with the ith radar. Its value is a continuous natural number, representing different jamming patterns;

- Considering the mathematical model of multi-object jamming resource scheduling, the constraint conditions are set as.

$$\begin{cases} \sum_{i=1}^{N} p_{ji} = 1, j = 1, 2, \cdots, M \\ s_{1i} = s_{2i} = \cdots = s_{ji} = \cdots = s_{Mi} \end{cases} \quad (9)$$

Where $\sum_{i=1}^{N} p_{ji} = 1$ indicates that the sum of the normalized jamming power of a jammer is 1. $s_{1i} = s_{2i} = \cdots = s_{ji} = \cdots = s_{Mi}$ means that the jamming patterns used by the jammers are all the same jamming pattern when jamming the same radar;

– **Step 1: Reproduction and Update:**

- Before starting the optimization, first set the population optimal solution set EP as an empty set ϕ. Then set a set of ideal points $z = (z_1, z_2, \ldots, z_i, \ldots, z_N)$, z_i denotes the ith ideal point. Randomly initialize all ideal point values according to constraint conditions, and define a set of weight vectors $\lambda^1, \ldots, \lambda^k, \ldots \lambda^K$. Where, λ^k represents the kth weight vector, K is the population size;
- Euclidean distance is used to calculate the T neighboring vectors that are closest to each weight vector. Calculate the Euclidean distance between the adjacent weights, and the$T$ vectors closest to the weight vector λ^k are the adjacent vectors of the weight vector λ^k. Where the adjacent vectors index set is denoted as $B(k) = (k_1, \ldots, k_T)$, $\lambda^{k_1}, \lambda^{k_2}, \ldots, \lambda^{k_T}$ is the T adjacent vectors of λ^k;
- Generate the initial population weight vector set $P = \{x^1, \ldots, x^k, \ldots x^K\}$, $x \in \Theta$. Sample from the decision space Θ uniformly and randomly. Where, x^k represents the kth weight vector of the population, and the initial k value is set to 1;

- Select two indexes m, n arbitrarily from the set $B(k) = (k_1, \ldots, k_T)$ of adjacent vector indexes, and implement the crossover operation based on the standard genetic algorithm on x^m and x^n to obtain a new individual y;
- Perform mutation operation based on standard genetic algorithm on the new individual y to get the mutated individual $y^{'}$;
- Update the ideal point: if $z_w < f_w\left(y^{'}\right)$, $w = 1, \ldots, N$, then $z_w = f_w\left(y^{'}\right)$;
- Update the adjacent solution: If $y^{'}$ is better than x^w which is any one of $B(k)$ (measured by the fitness of the kth subproblem), then x^w is replaced by $y^{'}$. That is, for $w \in B(k)$, if $g^{pbi}\left(y^{'}|\lambda^w, z\right) \le g^{pbi}(x^w|\lambda^w, z)$, then $x^w = y^{'}$, $z_w = f_w\left(y^{'}\right)$.Where, g^{pbi} represents the decomposition operation based on improved penalty boundary intersection;
- Judge $F\left(x^k\right)$, $k = 1, \ldots, K$ whether it is dominated by $F\left(y^{'}\right)$: if dominated, $F\left(x^k\right)$ will be removed from the population optimal solution set EP. For $\forall i = 1, \cdots, N$, if there is no dominance, $F\left(y^{'}\right)$ will be added to the population optimal solution set EP, and the value of k increased by one.

– **Step 2: Stopping Criteria:**

- Repeat the last five steps of **Step 1** until $k = K$, the population optimal solution set EP after evolution is obtained, and the population optimal solution set EP contains the jamming style decision result $s_1^{opt}, s_2^{opt}, \ldots, s_i^{opt}, \ldots, s_N^{opt}$ and the jamming power decision result p_{ji}^{opt}, $j = 1, \ldots, M$, $i = 1, \ldots, N$. Where, s_i^{opt} represents the jamming pattern adopted to interfere with the ith radar, and p_{ji}^{opt} represents the jamming power applied by the jth jammer to the ith radar.

– **Step 3: Output:**

- According to the optimal distributed jamming method obtained in **Step 2**, consider that each jammer J_j in the set $J = \left[J_1, J_2, ..., J_j, ..., J_M\right]$ adopts an jamming pattern s_i^{opt} to transmit jamming signals to the ith radar for the jamming power p_{ji}^{opt}, and finally complete the distributed jamming to the other radar network.

4 Simulated Experiments

4.1 Experimental Settings

The space confrontation scene is shown in Fig. 1. In order to validate the effectiveness of the proposed approach, the simulation condition is set as the total number of radars to 3, the distributed jamming network contains 8 jammers, the number of neighbors of the multi-target evolutionary algorithm decomposed by PBI is 200, the crossover probability is 0.5, the mutation probability is 0.5, and the crossover operator used in this paper is simulate binary crossover (SBX), its crossover mutation parameter is 1. The mutation operator parameter is 1, the external population output threshold is 200, and the maximum number of iterations is 200. The bandwidth of the STAP radar is 20 MHz, the carrier frequency is 1.5 GHz, the number of array elements is 12, and the number of pulses is 24.

The settings of above simulation condition are summarized as follows (Table 1).

Table 1. Experimental simulation parameters configuration

Parameters style	Configuration information
Number of radars	3
Number of jammers	8
Number of neighbors	200
Crossover probability	0.5
Mutation probability	0.5
SBX crossover mutation	1
Mutation operator	1
External population output	200
Maximum number of iterations	200
Bandwidth of the STAP radar	20 MHz
carrier frequency	1.5 GHz
Number of array elements	12
Number of pulses	24

In the case of jamming from the mth jammer to the nth radar, we define the jamming power allocation matrix P_{JR}. As shown in formula (10), the jamming power allocation matrix represents the power allocated when the mth jammer interferes with the nth radar.

$$P_{JR} = \begin{bmatrix} p_{11} & p_{12} & \cdots & p_{1N} \\ p_{21} & p_{22} & \cdots & p_{2N} \\ \cdots & \cdots & p_{mn} & \cdots \\ p_{M1} & p_{M2} & \cdots & p_{MN} \end{bmatrix} \tag{10}$$

In addition, conditional constraints on the jammer include the same jammer can only interfere with up to 3 radars at the same time; the sum of the normalized power of the jammer is 1. And conditional constraints on radars include each radar is jammed by at least one jammer; when jamming the same radar, the jammers use the same jamming pattern.

4.2 Experimental Results

Now use the above experimental parameters to optimize the multiobjective problem. The decision optimization result is the normalized power allocation scheme of the jammer in the many-to-many confrontation.

Table 2 shows the normalized power allocation scheme of jammers obtained by optimization. Where taking the first line as an example, it represents that the normalized power allocated by jammer 1 to radar 1, radar 2, and radar 3 are 0.23, 0.05, and 0.72, respectively. In order to observe the tendency of jamming power resource allocation more intuitively, the statistical results shown in the table are drawn into power distribution diagram, as shown in Fig. 4. Since the solution obtained by the multiobjective optimization algorithm is a non-dominated solution, the optimization result is not unique.

Table 2. Power distribution

	Radar 1	Radar 2	Radar 3
Jammer 1	0.23	0.05	0.72
Jammer 2	0.15	0.26	0.59
Jammer 3	0.34	0.14	0.52
Jammer 4	0.38	0.02	0.60
Jammer 5	0.13	0.23	0.64
Jammer 6	0.20	0.09	0.71
Jammer 7	0.49	0.11	0.41
Jammer 8	0.05	0.32	0.63

It can be seen from Fig. 4 and Table 2 that most jammers allocate most of the power to radar 3, which is consistent with the degree of jamming power set in the scene. Since radar 1 and radar 2 have similar threat levels, there is a situation of competing for the remaining jamming resources, which is also consistent with the actual setting. It shows that the allocation scheme of jamming resources obtained from optimization is reasonable to a certain extent.

After verifying the rationality of the multi-objective optimization scheme, the effectiveness of the obtained jamming resource allocation scheme will be verified. The jamming power is allocated as Table 2, and the rest of the simulation parameters remain unchanged as above.

Under above simulation conditions, comparing jamming signals not optimized by improved MOEA/D-PBI, and jamming signals obtained by the present invention to interfere with STAP radar. The output improvement factor statistical graphs are shown in Fig. 5, Fig. 6 and Fig. 7, respectively.

From the comparison graphs of the improvement factors of three radars, it can be seen that the radar 3 with the highest jamming threat level obtains the most jamming resources, and the notch in the improvement factor is enlarged, and the decline is the most obvious. It proves that the optimized jamming decision-making program by the improved MOEA/D-PBI algorithm is more flexible and can be adjusted strategically and adaptively according to the threat level of the battlefield target. Meanwhile, the improvement factors of radar 2 and radar 1 have the second highest jamming threat level, and have also been reduced to varying extent.

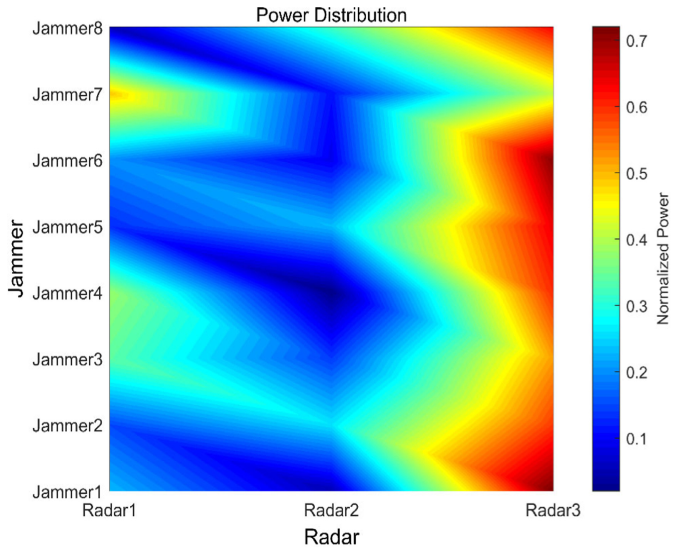

Fig. 4. Illustration of Power Distribution.

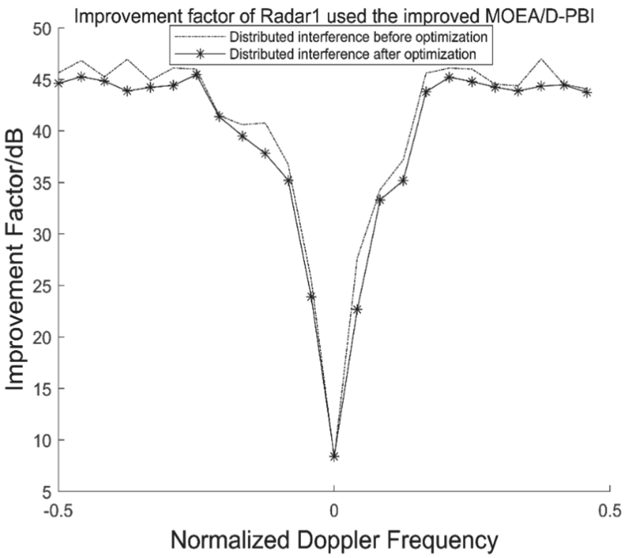

Fig. 5. Improvement factor of Radar 1 with the improved MOEA/D-PBI.

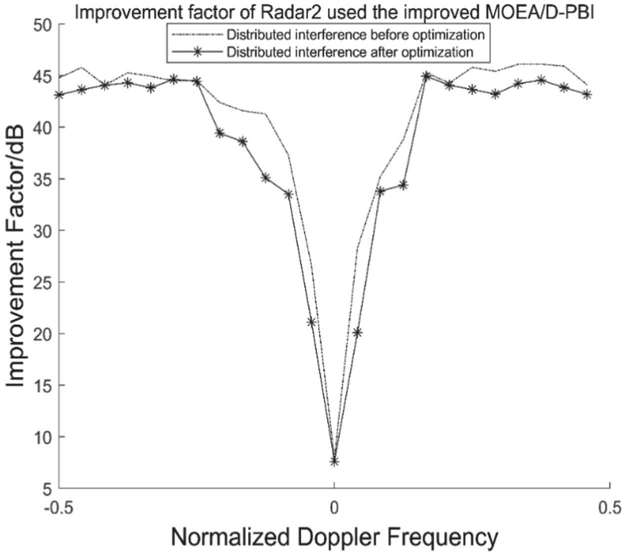

Fig. 6. Improvement factor of Radar 2 with the improved MOEA/D-PBI.

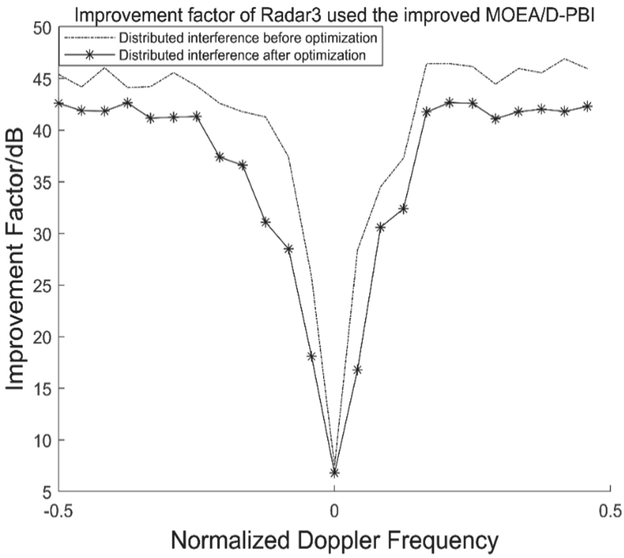

Fig. 7. Improvement factor of Radar 3 with the improved MOEA/D-PBI.

5 Conclusions

Due to competition among various radars and preemptive jamming resources, it is difficult to find a unique solution to optimize the jamming effects of all radars at the same time. Based on the above situation, a new distributed jamming optimization scheme based on improved MOEA/D-PBI algorithm is proposed to solve multiobjective function values in this paper, and the optimal solution set can achieve the balance among the objective functions. It can be seen from the simulation results that the optimization scheme obtained by the optimization algorithm is reasonable, and the power of the jammer can be distributed more obliquely according to the actual radar threat level, which is consistent with the actual environment settings. Finally, through simulation experiments, the optimized distributed jamming scheme is compared with the distributed jamming scheme before optimization, verifying the feasibility of the distributed jamming optimization scheme proposed in this paper, which can effectively interfere with radar in multiobjective situation.

References

1. Guerci, J.R.: Space-time Adaptive Processing for Radar. Boston: Artech House, pp. 23–38 (2003)
2. Melvin, W.L.: A STAP overview. IEEE AES Mag. **19**(1), 19–35 (2004)
3. Klemm, R.: Principles of Space-time Adaptive Processing: Inst Elect Eng, pp. 22–39. London, U.K (2002)
4. Commander, C.W., Pardalos, P.M., Ryabchenko, V.: The wireless network jamming problem. J. Comb. Optim. **4**, 481–498 (2007)
5. Chen, J., Zhang, Q., Li, G.: MOEA/D for multiple multi-objective optimization. In: Ishibuchi, H., et al. (eds.) EMO 2021. LNCS, vol. 12654, pp. 152–163. Springer, Cham (2021). https://doi.org/10.1007/978-3-030-72062-9_13
6. Sato, H.: Adaptive update range of solutions in MOEA/D for multi and many-objective optimization. In: Dick, G., et al. (eds.) SEAL 2014. LNCS, vol. 8886, pp. 274–286. Springer, Cham (2014). https://doi.org/10.1007/978-3-319-13563-2_24
7. Li, H., Zhang, Q.: Multiobjective optimization problems with complicated pareto sets, MOEA/D and NSGA-II. IEEE Trans. Evol. Comput. **12**(2), 284–302 (2009)
8. Zhang, Q., Li, H.: MOEA/D: a multiobjective evolutionary algorithm based on decomposition. IEEE Trans. Evol. Comput. **11**(6), 712–731 (2007)
9. Das, I., Dennis, J.E.: Normal-bounday intersection: a new method for generating Pareto optimal points in multicriteria optimization problems. SIAM J. Optim. **8**(3), 631–657 (1998)
10. Messac, A., Ismail-Yahaya, A., Mattson, C.: The normalized normal constraint method for generating the Pareto frontier. Struct. Multidisc. Optim, **25**, 86–98 (2003)
11. Guo, J., Yang, S., Jiang, S.: An adaptive penalty-based boundary intersection approach for multiobjective evolutionary algorithm based on decomposition. In: 2016 IEEE Congress on Evolutionary Computation (CEC), pp. 2145–2152 (2016)
12. Li, H., Sun, J., Zhang, Q., Shui, Y.: Adjustment of weight vectors of penalty-based boundary intersection method in MOEA/D. In: Deb, K., et al. (eds.) EMO 2019. LNCS, vol. 11411, pp. 91–100. Springer, Cham (2019). https://doi.org/10.1007/978-3-030-12598-1_8